Parametric study and optimization of the cryo-magnetic system for EU DEMO at the pre-conceptual design phase

Christine Hoa, Thomas Latella, François Bonne, Benoît Lacroix, Quentin Le Coz, Louis Zani, Monika Lewandowska, Kamil Sedlak, Valentina Corato

Version of Record: https://www.sciencedirect.com/science/article/pii/S0011227522000571
Manuscript_e26abc9ad09a1e9a62abd3ddcc83df41

Parametric study and optimization of the cryo-magnetic system for EU DEMO at the pre-conceptual design phase

Christine Hoa[a], Thomas Latella[a], François Bonne[a], Benoît Lacroix[b], Quentin Le Coz[b], Louis Zani[b], Monika Lewandowska[c], Kamil Sedlak[d], Valentina Corato[e].

[a]*Univ. Grenoble Alpes, CEA IRIG-SBT, Grenoble 38000 France*

[b]*CEA IRFM, Saint Paul lez Durance 13018 France*

[c]*Faculty of Mechanical Engineering and Mechatronics, West Pomeranian University of Technology, Szczecin, Poland*

[d]*École Polytechnique Fédérale de Lausanne (EPFL), Swiss Plasma Center (SPC), Forschungsstrasse 111, 5232 Villigen PSI, Switzerland*

[e]*ENEA, ENEA C.R. Frascati, 00044 Frascati (Rome), Italy*

Author mail address: christine_hoa@yahoo.com

Abstract

The pre-conceptual design phase of the EU DEMO magnet system relies on mechanical, electromagnetic and thermal-hydraulic analyses of different conductor designs for the Toroidal Field (TF) coils, the Poloidal Field (PF) coils and the Central Solenoid (CS) magnet. The cryo-magnetic system includes the superconducting magnets cooled by forced flow of supercritical helium at about 4.5 K, the cryo-distribution lines and valve boxes, and the cryogenic system with several cold boxes. The present analysis focuses on the cooling requirement of the TF coils with three winding pack options for the cable in conduit conductors based on 2015 DEMO baseline, featuring pancake or layer winding approaches. This analysis methodology would be further developed with the latest conductor designs and more complete heat load assumptions for the future conductor design studies and the specification of the cooling requirements. Parametric studies on the cold source temperature and on the supercritical helium mass flow rate have been performed on the three conductor designs in order to identify for each one the impact of the cooling conditions onto the temperature margin with respect to the current sharing temperature. In this study, the heat load contribution have been limited to the estimation of the neutron heating and some joint resistance heat loads when available. In addition, Simcryogenics, a dynamic modelling tool developed by CEA, is used to model supercritical helium loops for cooling different conductor designs. An algorithm has been developed to optimize both the cold source temperature and the supercritical helium mass flow, in order to minimize refrigeration power for each conductor design. Optimization studies are analyzed and compared in order to estimate for each TF winding pack design, the impact on refrigeration power. The interest of such quick cross-check analyses is to identify design improvements for the conductors and the cryo-distribution, keeping acceptable temperature margins and minimizing the refrigeration power.

Keywords: Fusion, EU DEMO, Cryo-magnetic system, dynamic modelling, optimization algorithm

1 Introduction

The European DEMO is a future demonstration fusion reactor entering its conceptual design (2021-2025). The future reactor would be a 2 GW class machine, with large superconducting coils; capable to demonstrate the production of electricity and to operate in a closed fuel cycle. Its size would be roughly1.5 times the size of ITER, with a major and minor radius of 9.1 and 2.9 m, respectively and an on axis magnetic field of 5.3 T,

resulting in a peak field on the toroidal field conductor of 12.0 T [1, 2, 3]. The low temperature superconductors (LTS) remains the baseline technology solution for the superconducting magnets and several conductor options have been investigated during the pre-conceptual design phase for each magnet system. Extensive mechanical, electromagnetic, thermal hydraulic analyses on the superconducting magnet conductors have been performed during a pre-conceptual design phase in the framework of the EUROfusion collaboration, involving several European laboratories [4, 5, 6, 7, 8]. All the superconducting magnets have been investigated: 16 toroidal field coils, 5 central solenoid modules, 6 poloidal field coils. The present analysis focuses on the cooling requirement of the TF coils with three winding pack options for the cable in conduit conductors based on 2015 DEMO baseline [6]. The winding packs WP1 [9] and WP2 [10] are innovative based on react and wind NB_3Sn technology featuring a winding of the coils in layers, allowing a graded conductor approach, with different conductor characteristics depending on the layer position with respect to the thermal loads and the magnetic field maps. Such approach allows for significant savings of superconductor material amount and cost. A third winding pack WP3 option [11], similar to the ITER TF concept, benefits from the manufacturing experience of the wind and react conductors. In this concept, the coils are wound in double pancakes and only one conductor type is designed to fulfill the mechanical, electromagnetic and thermal-hydraulics requirements of all the 8 double pancakes.

Previous studies on optimization on the cooling requirement [12] and the overall cost of the cryo-magnet system [13] have highlighted the interest to have models and simulation methods to check the conductor performance in terms of temperature margin with respect to the current sharing temperature T_{cs}. The cold source temperature and the supercritical helium mass flow rate are the two main parameters to investigate for each of conductor designs. The analysis will present the methodology applied with Simcryogenics, a dynamic modelling tool developed by CEA [14]. The simulation tool is well suited to perform quick thermal hydraulic calculations for modelling different conductor designs cooled by supercritical helium loops in forced flow convection. An algorithm has been developed to optimize both the cold source temperature and the supercritical helium mass flow, in order to minimize the refrigeration power for each conductor design.

After the presentation of the thermal hydraulic models for the three TF winding pack options, the optimization methodology based on the minimization of the refrigeration power is introduced and detailed. The optimization studies on the resulting input power for an ideal refrigerator at 300 K are analyzed and compared for each TF winding pack design, highlighting the main differences for the layer and the pancake designs. The interest of such quick cross-check analyses is to identify design improvements for the conductors and the cryo-distribution, keeping acceptable temperature margins and minimizing the ideal refrigeration power.

2 Thermal-hydraulic model description and assumptions

2.1 Cable in Conduit Conductor designs

Three TF cable-in-conduit conductor (CICC) designs have been modelled, with the 2015 DEMO data and are illustrated in Figure 1. There are two innovative options with layer wound designs and one option with pancake wound conductor which is the “ITER-like” design.

- WP1 (SPC) design: 12 single layers (Ls) wound using flat multistage cables with two side equilateral triangle cooling channels and one rectangular cooling channel [9] (Figure 2). Conductors in all layers are made of Nb_3Sn. This is a graded WP design: each layer is a different conductor type, with different amount of superconductor to comply with the magnetic field constraints and nuclear loads.
- WP2 (ENEA) design: 6 double layers (DLs) wound using rectangular CICCs with two cooling channels delimited from the bundle region with steel spirals [10] (Figure 3). The five inner DLs, located in the high magnetic field (HF) region, are made of Nb_3Sn conductors, while the most outer DL6 in the low field region (LF) is made of a Nb-Ti conductor. This is a graded WP design.
- WP3 (CEA) design (v2b) 8 double pancakes (DPs) wound using a square CICC with a central cooling channel delimited from the bundle region with a steel spiral [11] (Figure 4). All DPs are made of the same Nb_3Sn conductor.

The conductors’ parameters, relevant for the present analysis, are compiled in Tables 1, 2 and 3. We assumed that all channels of flow (i.e. the bundle regions and the cooling channels of all conductors) are connected hydraulically in parallel.

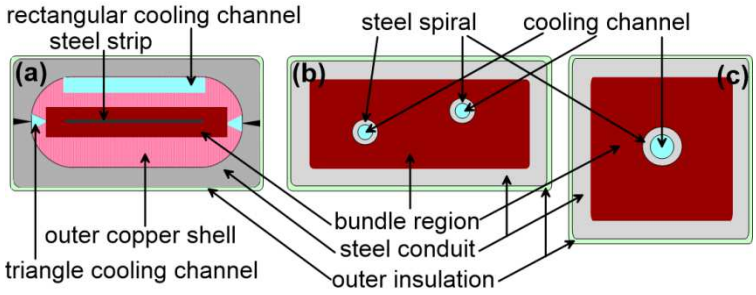

Figure 1: Views of the DEMO 2015 superconductor CICC (a) WP1 (b) WP2 (c) WP3

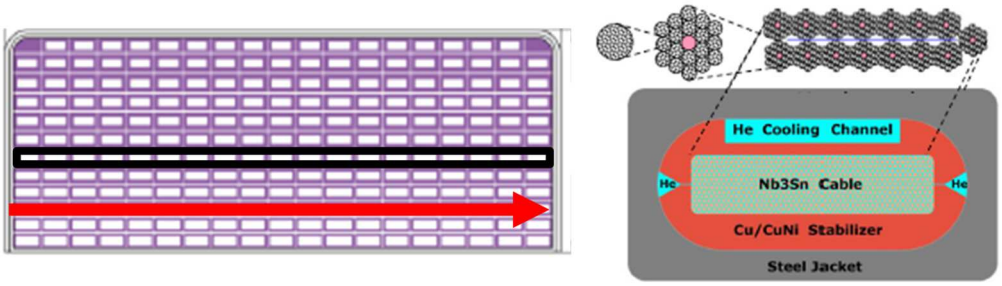

Figure 2: WP1 2015 design [9]

Table 1: Conductor parameters used in the analysis for WP1

Layer No.	Conductor length L (m)	Central bundle region								Single side triangle channel		Rectangular channel	
		φ (–)	$N_{sc\,str}$	$N_{Cu\,str}$	D_{str} (mm)	Steel strip dimensions (mm)	Bundle dimensions (mm)		A_{He} (mm^2)	D_h (mm)	A_{He} (mm^2)	D_h (mm)	A_{He} (mm^2)	D_h (mm)
L1	847	0.202	252	14	1.2	30 x 0.2	9.8	40.3	79.4	0.54	8.0	2.48	140	7.18
L2	851	0.201	288	16	1.0		8.2	38.4	63.1	0.45				
L3	855	0.200	288	16	0.9		7.4	34.6	51.1	0.40			140	7.18
L4	860	0.199	252	14			7.4	30.2	44.7	0.40			120	7.06
L5	864	0.199	174	29	1.0		5.1	41.3	42.1	0.42			115	7.02
L6	869	0.198	150	25			5.1	35.6	36.3	0.42			95	6.85
L7	874	0.198	126	21	1.0	25 x 0.2	5.1	29.9	30.5	0.42			85	6.73
L8	879	0.197	138	23	0.9		4.6	29.5	27.0	0.38			70	6.51
L9	884	0.197	132	22	0.9		4.7	28.2	25.9	0.38			60	6.32
L10	889	0.197	126	21			4.7	26.9	24.7	0.38			50	6.06
L11	894	0.196	120	20	0.9		4.7	25.7	23.5	0.37			40	5.71
L12	804	0.196	114	19			4.7	24.4	23.5	0.37				

The wetted perimeter for WP1 conductors is calculated using the following formula:

$$P_w = g(\varphi)\left[\pi\left(N_{sc\,str} + N_{Cu\,str}\right)D_{str}\frac{\cos\theta + 1}{2\cos\theta} + P_{strip} + P_{cable\,space}\right] \quad \text{(Eq. 1)}$$

where :

$\cos\theta = 0.976$

$g(\varphi) = \min(\varphi/0.4, 1)$ represents the assumed dependence on the void fraction φ.

P_{strip} is the wetted perimeter of the steel strip

$P_{cable\ space}$ is the wetted perimeter of the cable space

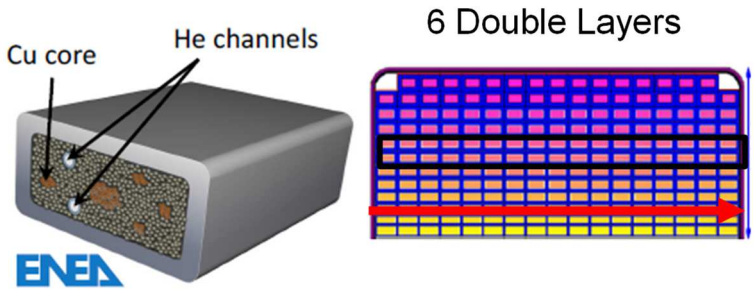

Figure 3: WP2 2015 design [10]

The white corners, illustrated on TF cross section, are not used as cooling channels and are filled with a resin.

Table 2: Conductor parameters used in the analysis for WP2

DL No.	Conductor No.	Conductor length L (m)	Bundle region								Single cooling channel				
			φ (–)	$N_{str\,(sc+Cu)}$	D_{str} (mm)	$N_{segr\,Cu}$	D_{Cu} (mm)	Bundle dimensions (mm)		A_{He} (mm^2)	D_h^{**} (mm)	A_{He} (mm^2)	D_{in} (mm)	D_{out} (mm)	Open area (%)	Spiral width (mm)
1	L1	747	0.27	720 + 360	1.0	108	1.5	61.1	26.0	405	0.57	19.6	5	7	40	5
	L2	751														
2	L3	755	0.25	360 + 720		54		58.3	24.3	330	0.54					
	L4	759														
3	L5	763	0.25	270 + 540		162		55.3	25.0	322	0.58					
	L6	768														
4	L7	772	0.25	180 + 630		108		52.1	24.0	287	0.56					
	L8	777														
5	L9	782	0.25	120 + 960		0		48.9	26.2	292	0.52					
	L10	788														
6	L11	794	0.29	972 + 0		108		45.5	33.2	415	0.59					
	L12	706														

The wetted perimeter for the WP2 conductors is calculated using the formula:

$$P_w = g(\varphi)\left[\pi\left(N_{str(sc+Cu)}D_{str}\frac{\cos\theta_1+1}{2\cos\theta_1}+N_{Cu}D_{Cu}\frac{\cos\theta_2+1}{2\cos\theta_2}\right)+P_{o,wrap}+2P_{o,spiral}\right] \quad \text{(Eq. 2)}$$

where $\cos\theta_1 = 0.97$ and $\cos\theta_2 = 0.99$ for strands with diameter 1 mm and 1.5 mm, respectively. $P_{o,wrap}$ is the wetted perimeter of the outer wrap located between the central bundle and the jacket. $P_{o,spiral}$ is the wetted perimeter of the spiral based on the outer diameter.

φ is the effective void fraction.

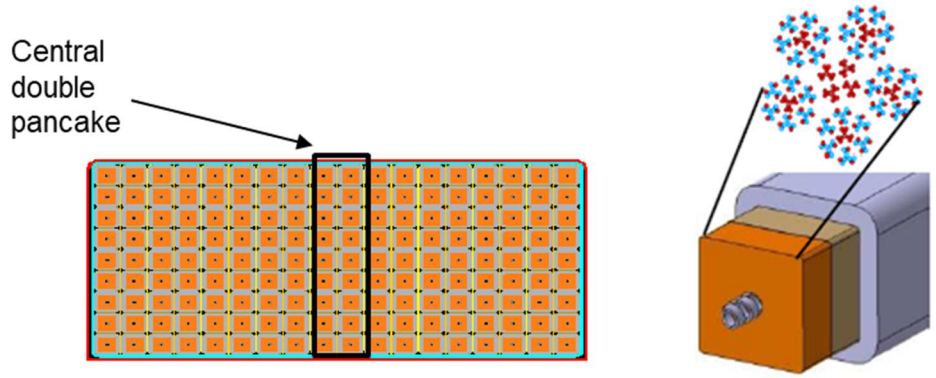

Figure 4: WP3 2015 design [11]

Table 3: Conductor parameters used in the analysis for WP3

Number of DPs	Conductor length L (m)	Bundle region						Central channel	
		φ (-)	$N_{str\,(sc+Cu)}$	D_{str} (mm)	A_{He} (mm^2)	Bundle dim. (mm)	D_h(mm)	D_{in} (mm)	D_{out} (mm)
9	408.18	0.288	828 + 790	0.984	524	43.62	0.55	8	10

The wetted perimeter for the WP3 conductors is calculated using the formula:

$$P_w = g(\varphi)\left[\pi D_{str}\left(N_{str\,sc} + N_{str\,Cu}\right)\frac{\cos\theta + 1}{2\cos\theta} + P_{o,wrap} + P_{o,spiral}\right] \quad \text{(Eq. 3)}$$

where $\cos\theta = 0.95$.

2.2 Fanning friction factor correlations

For the turbulent flow in the non-circular cooling channels of the WP1 conductors, the standard Bhatti –Shah friction factor correlations for the turbulent flow in straight smooth tubes [15] are used:

$$f_{BS\,turb} = 0.00128 + 0.1143\,\mathrm{Re}^{-0.311}\ ,\ \ 4000 < \mathrm{Re} < 10^7 \quad \text{(Eq. 4)}$$

For flows in the cooling channels of the WP2 conductors, the friction factor correlation obtained in [8] by CFD simulations has been applied:

$$f_{spiral1} = \frac{0.1687}{4\cdot \mathrm{Re}^{0.1129}}\ ,\ \ 2.5\cdot 10^4 < \mathrm{Re} < 1.5\cdot 10^5 \quad \text{(Eq. 5)}$$

For flows in the spiral central channel of the WP3 conductor, the empirical correlation has been used [6]:

$$f_{spiral2} = \frac{0.42}{4\cdot \mathrm{Re}^{0.1}} \quad \text{(Eq. 6)}$$

where Re are based on D_{out} .

To assess friction factors in the bundle region, the correlation based on the porous medium analogy model and the Darcy-Forchheimer momentum balance equation, taken from [16, 17], have been adopted:

$$f_{DF} = \frac{D_h^2 \varphi}{2K} \frac{1}{\mathrm{Re}} + \frac{D_h \varphi^2}{2} \frac{C_F}{\sqrt{K}} \quad \text{(Eq.7)}$$

where

$$K = 19.6 \cdot 10^{-9} \frac{\varphi^3}{(1-\varphi)^2} \text{ m}^2 \quad \text{(Eq. 8)}$$

$$\frac{C_F}{\sqrt{K}} = \frac{2.42}{\varphi^{5.80}} \text{ m}^{-1} \quad \text{(Eq. 9)}$$

2.3 Heat load assumptions

2.3.1 Nuclear heat loads

In a first approach, mainly focus on the optimization methodology and not directly on the optimized results, only the stationary nuclear heat loads have been taken into account. The assumption on the total heat load would be further improved by including also the stationary radiative and conductive loads and also the joule deposition in the joint resistances which would be estimated at the next conceptual design stage. The expected value of the nuclear heating load, $\dot{Q}$ (in W), deposited along the conductor due to neutron irradiation, was estimated by integrating the formula [17]:

$$P_{NH} = 50 \text{ W/m}^3 \cdot \exp(-r_{case}/0.140 \text{ m}) \quad \text{(Eq. 10)}$$

where r_{case} is the radial distance from the TF case plasma-facing edge.

We assume that in the layer wound coils (WP1 and WP2) the nuclear heat load is deposited evenly throughout each conductor, whereas in the pancake wound coil (WP3), heat deposited over each different turn is different. Thus the heat deposition per unit length of conductor $\dot{Q}_L$ is equal to:

For the WP1 and WP2 designs:

$$\dot{Q}_L = \dot{Q} / L \quad \text{(Eq. 11)}$$

for the WP3 design:

$$\dot{Q}_L(x) = \begin{cases} \dot{Q_{L1}} & \text{for } 0<x<L_1 \\ \dot{Q_{L9}} & \text{for } L_8<x<L \end{cases} \quad \text{(Eq. 12)}$$

where L_i is the coordinate of the end of the i^{th} turn and $\dot{Q}_{Li}$ is the heat deposition per unit length of conductor in the i^{th} turn (i = 1 .. 9). The heat transfer between the casing and the WP has not been taken into account, thus we assumed that the nuclear heating load deposited in the casing would be removed by a separate cooling circuit.

2.3.2 Inter-turn coupling

The Simcryogenic models of the CICC have taken into account the inter-turn coupling for the layer (for WP1), double layer (WP2) and pancake (WP3). In the conductive modelling, the stainless steel jacket and the insulation have been modeled with the assumptions illustrated in Figure 5 and summarized in Table 4.

Table 4: Inter-turn and inter-layer characteristics

	WP1	**WP2**	**WP3**
Number of layers or double layers or pancakes	12	12 (6 double layers)	18 (9 double pancakes)
Number of turn/layer or pancake	19	17	8
Jacket thickness inter-turn (inter-layer) (mm)	Grading [4.6; 9.1] ([5.7;11.4])	7.01	11.1
Insulation thickness inter-turn (inter-layer) (mm)	1 (2)	1 (2)	2

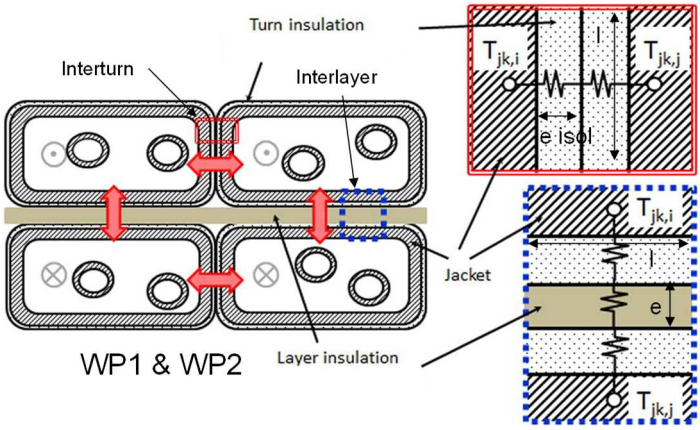

Figure 5: Inter-turn coupling and inter-layer coupling in WP2

(same principle applies for double layers in WP1 and pancake in WP3)

2.4 Supercritical helium loop model

The supercritical helium loop scheme (Figure 6) is modelled using the Simcryogenics library, as shown in Figure 7. This loop includes two heat exchangers immersed in a saturated helium bath, a cold circulator and 1D CICC based on the models described in section 2.2. The last stage of the refrigerator is modelled with a saturated helium bath, a Joule-Thomson (JT) expansion valve as well as a cold compressor. The boundary conditions for this last stage of the refrigerator are 10 bar and 4.5 K at the inlet of the JT valve and 1.3 bar at the outlet of the cold compressor. The isentropic efficiency of the cold compressor and circulator are considered to be equal to 0.7 for all operating conditions, as this study is not performed for a fixed but variable design of the cold compressor and circulator. The level and the pressure (and therefore temperature) of the saturated bath are regulated. The pressure at the inlet of the conductor as well as the pressure drop between its inlet and outlet are also regulated. The pressure at the inlet of the conductor is 6 bar while its inlet temperature is given by:

$T_{inlet\ CICC} = T_{bath} + \Delta T$ (Eq. 13)

With ΔT a constant value set to 0.05 K and T_{bath} the temperature of the saturated helium bath.

The refrigeration load representative of one TF coil is calculated with an enthalpy balance at the cold end of the refrigerator as shown on figure 6 and figure 7. The refrigeration loads for one TF magnet are obtained by summing the loads for each layers for WP1 and WP2. For WP3, only one pancake is simulated and the refrigeration loads are multiplied by the number of pancakes.

For WP1 and WP2:

$P_{refr,1\,TF} = \sum_{i=layers} \dot{m}_i \left(h_{2,\mathrm{LP,i}} - h_{1,\mathrm{HP,i}}\right)$(Eq. 14)

For WP3:

$P_{refr,1\,TF} = N_{pancake} * \dot{m} \ \left(\mathrm{h}_{2,LP} - h_{1,HP}\right)$ (Eq. 15)

With:

$P_{refr,1\,TF}$ refrigeration power at cold end of the refrigerator to cool 1 TF magnet

$N_{pancake}$ number of pancakes

$\dot{m}$ the mass flowrate flowing through the JT valve

$h_{1,HP}$ the specific enthalpy at the inlet of the JT valve

$h_{2,LP}$ the specific enthalpy at the outlet of the cold compressor

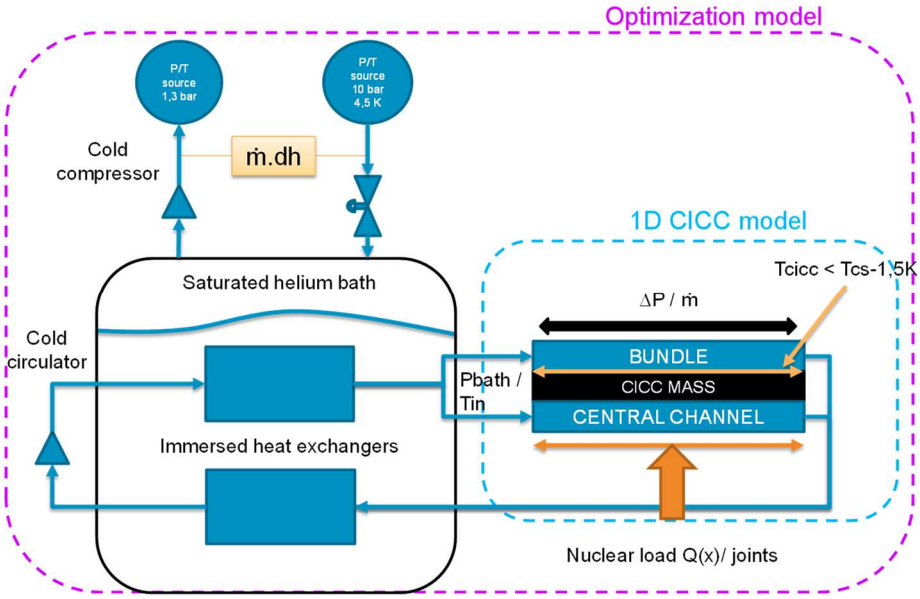

Figure 6: Supercritical helium loop modelling for optimization, including a 1D CICC model

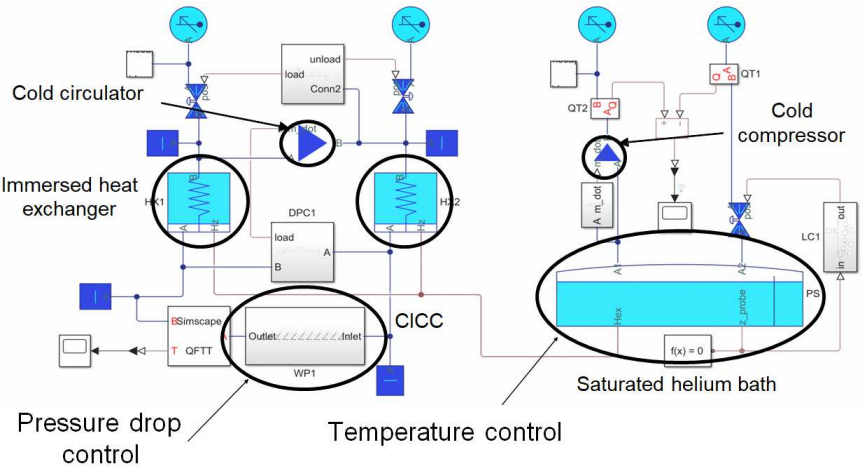

Figure 7: Simcryogenics model for the supercritical loop. The right part corresponds to the saturated helium bath and its interfaces to the refrigerator through the HP line with the Joule Thomson valve and through the LP line with the cold compressor (isentropic efficiency of 0.7). The left part of the representation correspond to the supercritical helium loop driven by a cold circulator (isentropic efficiency of 0.7), coupled to the saturated helium bath through the immersed heat exchangers. The two main controls are described: the pressure drop of the SHe loop and the temperature of the saturated bath (by the pressure of the bath). A level control is also implemented for the saturated bath with the Joule Thomson valve acting as the actuator.

For comparisons between the conductor designs, the input power of an ideal refrigerator at 300K is calculated based on the exergy balance:

WP1 and WP2:

$$P_{ideal,300K} = \mathrm{N}_{coils} \sum_{i=layers} \dot{m}_i \left(ex_{1,\mathrm{i}} - ex_{2,\mathrm{i}}\right) \quad \text{(Eq. 16)}$$

WP3:

$$P_{ideal,300K} = \mathrm{N}_{coils} * N_{pancake} * \dot{m}_{pancake}(ex_1 - ex_2) \quad \text{(Eq. 17)}$$

With:

$P_{ideal,300K}$ the input power of an ideal refrigerator at 300 K

$\dot{m}$ the mass flowrate flowing through the JT valve

ex_1 the specific exergy at the inlet of the JT valve with a reference temperature of 300 K

ex_2 the specific exergy at the outlet of the cold compressor with a reference temperature of 300 K

3 Optimization methodology to minimize the equivalent refrigeration power

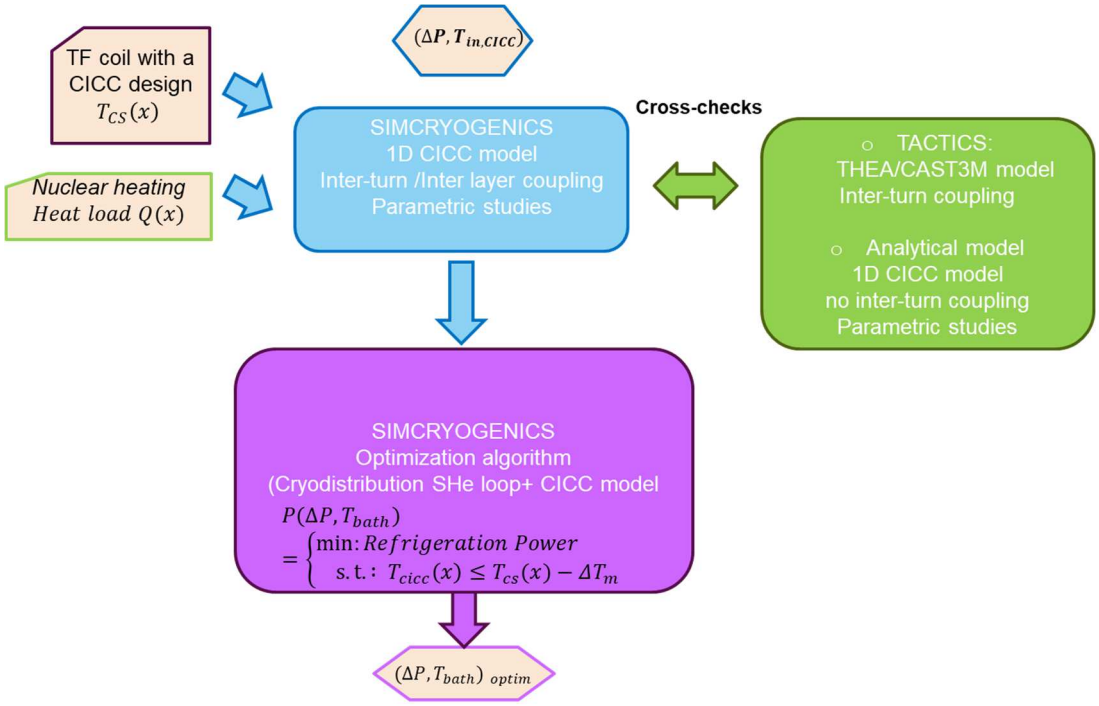

Figure 8: Methodology for optimization of refrigeration power, with the 2 parameters: pressure drop ΔP and inlet temperature of the conductor $T_{in,CICC}$

Figure 8 describes the methodology which has been followed to study the cooling requirement of a given TF conductor design (geometry and $T_{cs}(x)$), under a given spatial repartition of nuclear heating load $Q(x)$, with a given temperature constraint with respect to the current sharing temperature:

$$T_{cs}(x) - T_{CICC}(x) < \Delta T_m \quad \text{(Eq. 18)}$$

In our studies, the commonly accepted $\Delta T_m = 1.5\ K$ has been assumed [16].

The variables for the optimization algorithm are:

- $\Delta \boldsymbol{P}$, the pressure drop along the hydraulic length [0.2; 1 bar]. It is equivalent to an optimization on the mass flow as pressure drop and mass flow are directly linked to the hydraulic design of the conductor. The minimum pressure has been fixed to 0.2 bar as lower pressure drop would be too small compared to the total pressure head of the closed SHe loop and should be avoided to ensure a good control and sharing of the flow in the parallel conductor circuits. The maximum pressure drop of 1 bar is the reference pressure drop, commonly used in magnet design for fusion [16]. Higher values would lead to higher pumping power for the cold circulators.
- $\boldsymbol{T_{in,\,CICC}}$ the inlet temperature of the CICC [4.0; 4.6 K]. The minimum temperature has been fixed at 4.0 K to explore low values which can be easily reached with the current available cold compressor technology (pressure ratio possible with one or two stages of compressor). The maximum temperature is fixed at 4.6 K, which is reasonable maximum value with respect to the current sharing temperature of conductors.

The optimization method relies on the Simcryogenics tool developed by CEA, with a simplified conductor model including inter-turn and inter-layer coupling; and an optimization model including the cryo-distribution circuits up to the cold end of the refrigerator, previously presented in the section 2 (Figure 7). The optimized variable is the total refrigeration power, including both the loads deposited into the conductor and the loads required for the cryo-distribution (cold circulator and cold compressor). The optimization solver is minimizing the total refrigeration power, with the temperature margin $\Delta T_m = 1.5\ K$ and calculates the optimized interface parameters $(\Delta \boldsymbol{P}, \boldsymbol{T_{in,\,CICC}})$ between the cryo-distribution and the magnets.

For the parametric studies, four values have been chosen in the defined range: [4.05; 4.2; 4.35; 4.5] K and [0.25;0.5;0.75;1] bar. Two different tools have been used to map the cartography in terms of pressure drop and temperature:

- CEA TACTICS coupling THEA for thermal hydraulics of the CICC and Cast3M for 2D thermal modelling of the structures of the TF coil in the case of WP3 [19].
- Analytical model from WPUT [6, 20] assessing the temperature profile of 1D conductors for WP1 (12 layers), WP2 (6 double layers) and WP3 (1 pancake).

These parametric studies provide relevant results which could be cross checked with the calculated parameters obtained with the optimization tool. Indeed, they provided also some additional information on the sensitivity of the total refrigeration with respect to the variations of the inlet temperature and the pressure drop.

Figure 9 gives the comparative results for the WP2 design, on the four first odd layers, for both the Simcryogenics simplified model and the analytical model from WPUT. The temperature margins calculated by the two models are in good agreement for the layers L5, L7 which are less loaded (15.1 W and 8.7 W respectively). Some discrepancies can be noted for the layers L1 and L3 which are the most loaded (39.6 W and 23.6 W respectively): Simcryogenics predicts higher or lower temperature margin for these two layers. The inter-turn thermal coupling modelled by Simcryogenics, which is not taken into account by the analytical model, could explain the differences, related to a more peaked heat load distribution for L1 and L3 assumed with the analytical model.

After having cross checked the Simcryogenics simplified model with the analytical model from WPUT and with the 2D modelling of the CICC, the relatively good agreement of the results of the parametric studies, lead us to use the Simcryogenics model as an input to the optimization algorithm presented in Figure 8.

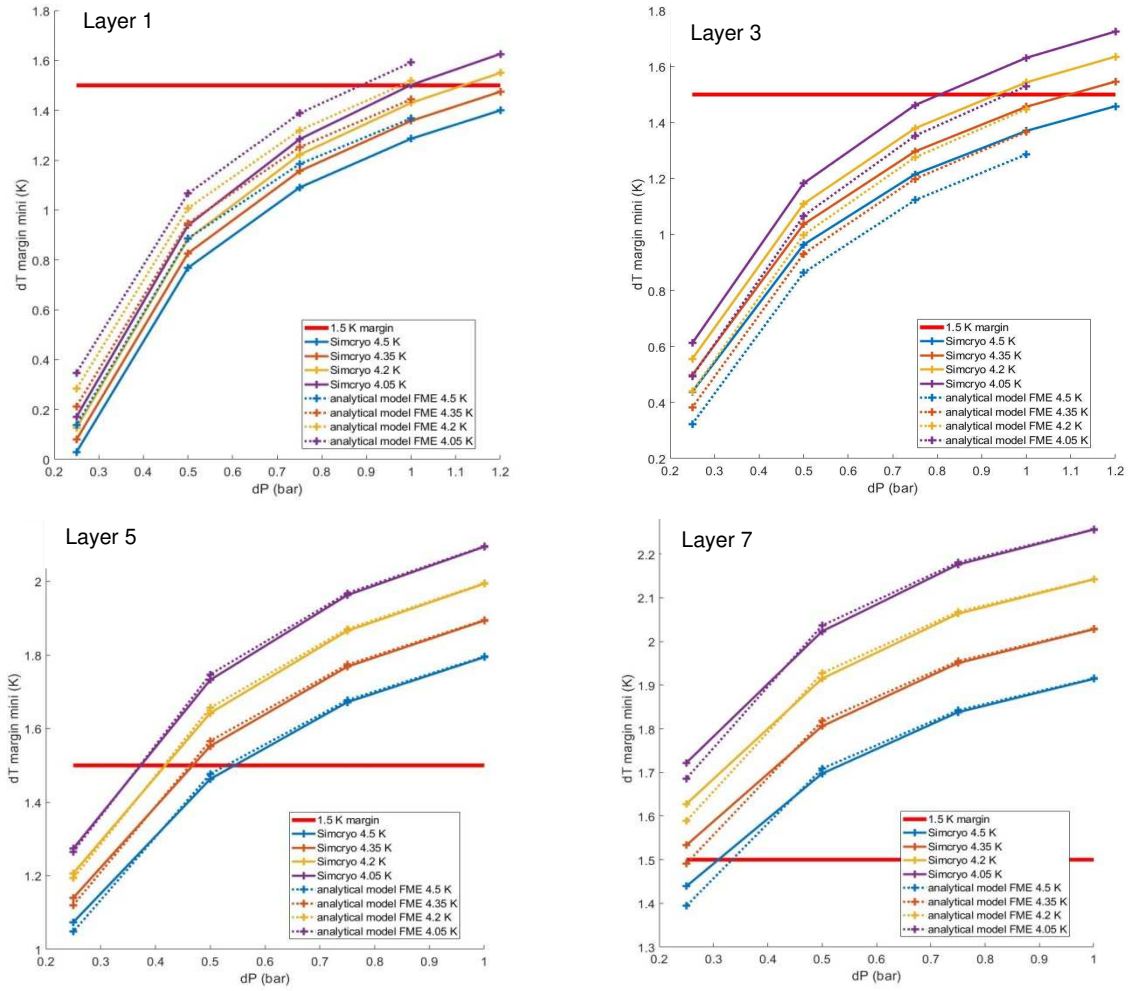

Figure 9: Parametric study comparisons with Simcryogenic and the analytical model from WPUT, on the WP2 design for the six odd layers: temperature margin results with varying pressure drop and inlet temperature

4 Comparative results

The optimization algorithm has been applied to the three TF winding pack designs, in order to identify for each TF design, the optimized set of parameters ($\Delta \boldsymbol{P}, \boldsymbol{T_{in,\,CICC}}$), which will minimize the input power of an ideal refrigerator at 300 K, with the given constraint on the temperature margin of 1.5 K with respect to the current sharing temperature. Another interesting result is the comparison with the reference parameters defined as ($\Delta \boldsymbol{P}$=1 bar, $\boldsymbol{T_{in,\,CICC}}$=4.5 K), which are the commonly used conductor design parameters for ITER and for JT-60SA conductors [21]. The comparisons will allow to quantify the impact of the cooling requirement ($\Delta \boldsymbol{P}$, $\boldsymbol{T_{in,\,CICC}}$), between the refrigeration powers (enthalpy balance) $P_{refr,\,reference}$ and $P_{refr,\,optimized}$, depending on the conductor designs. The heat loads mentioned in the table 5, 6 and 7 correspond to the input power to the coils (nuclear heat loads, except for WP2 which also includes joint resistance joule heating).

4.1 Layer designs

Table 5 shows the optimization results for WP1, based on the model including the 12 layers, thermally coupled. The optimized cooling scheme would supply helium at 4.6 K, with a pressure drop of 0.48 bar. It would reduce the refrigeration power by 33% compared to the reference case (4.5 K and 1 bar).

Table 5: Optmization results for WP1

ΔP (bar)	0.48
T_{inlet} (K)	4.6
$P_{refr,\ reference}$(W)	342
$P_{refr,\ optimized}$ (W)	229
Power saving (%)	-33
Heat loads (W)	186

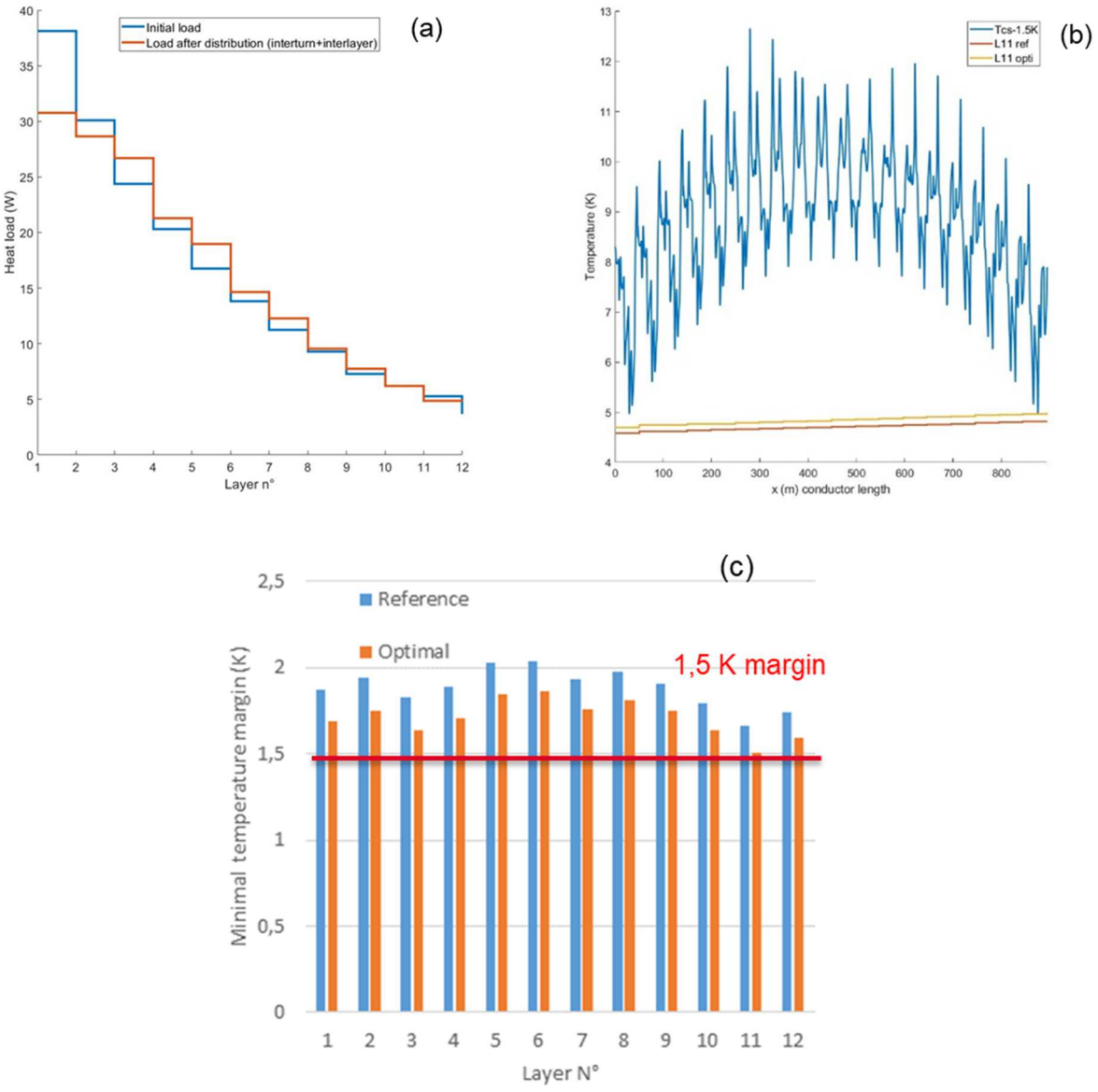

Figure 10: Optimization results for WP1: heat load repartition (a), conductor temperature profile for layer 11 (b), calculated minimum temperature margins for the 12 layers with comparison with the reference case (c).

Looking at the temperature profiles (Figure 10b) and temperature margins with respect to the current sharing temperature (Figure 10c), the layer L11 is the most critical: the temperature margin of 1.5 K is reached at the end of the conductor length. The other layers have temperature margin higher than 1.5 K up to 2.0 K for L5 and L6. One has to note that in the reference case (4.5 K and 1 bar pressure drop), all the layers comply with a temperature margin higher than 1.5 K, even higher than 1.6 K (L11). The WP1 design with the reference cooling parameters (4.5 K, 1 bar pressure drop) has additional margin with respect to the 1.5 K temperature margin. The impact of the inter-layer coupling (Figure 10a) is not negligible as the heat loads are re-distributed and L1 and

L2 have lower heat loads, whereas the other layers are more loaded. With cooling parameters of 4.6 K and 0.48 bar pressure drop, WP1 would be more optimized in terms of refrigeration power (-33%).

Table 6 shows the optimization results for WP2, based on model including the 6 double layers, thermally coupled. The optimized cooling scheme would supply helium at 4.05 K, with a pressure drop of 1.0 bar. It would increase the refrigeration power by +25% compared to the reference case (4.5 K and 1 bar).

Table 6: Optimization results for WP2

ΔP (bar)	1.0
T_{inlet} (K)	4.05
$P_{refr,\ reference}$(W)	217
$P_{refr,\ optimized}$W)	271
Power saving (%)	+25
Heat loads (W)	167

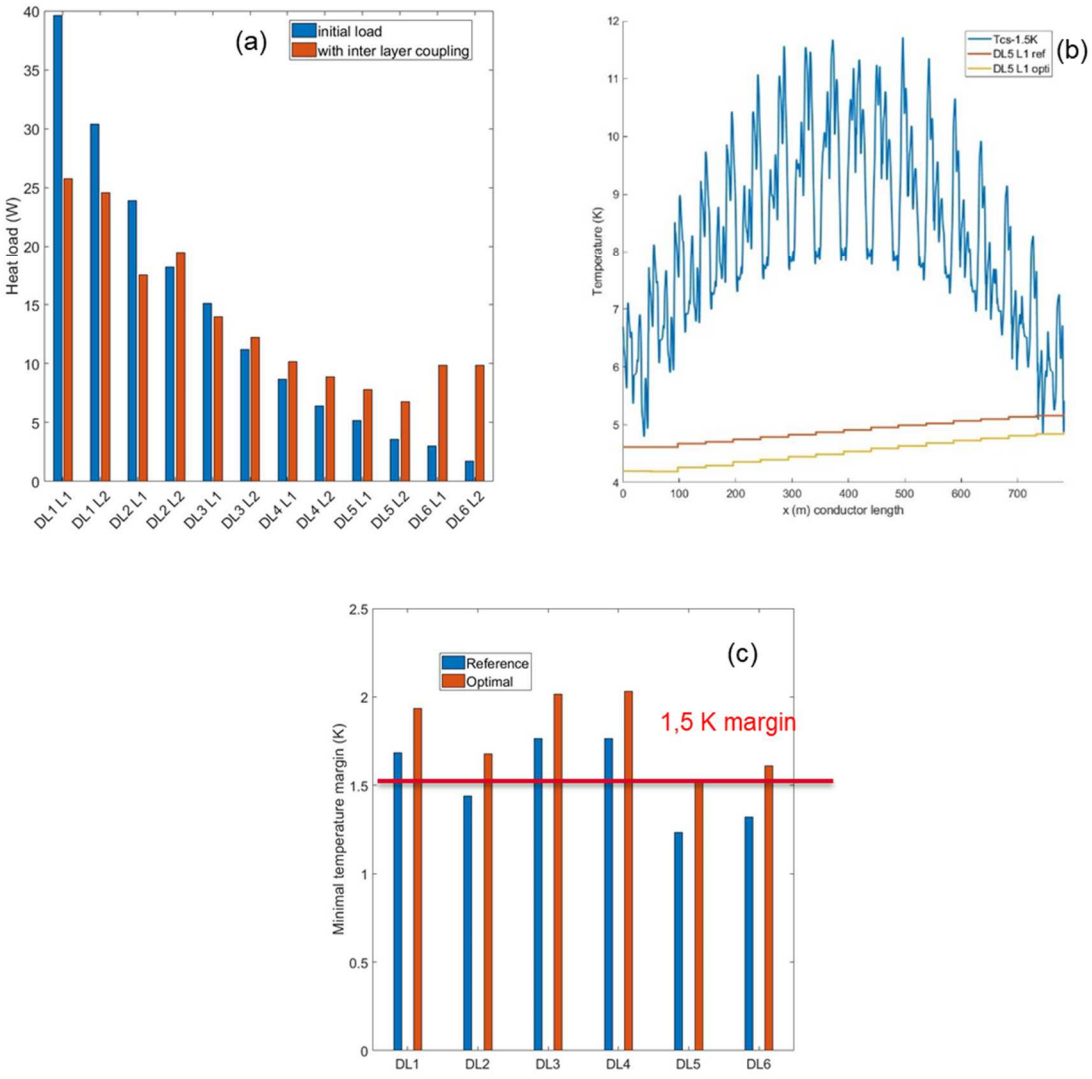

Figure 11: Optimization results for WP2: heat load repartition (a), conductor temperature profile for layer 11 (b), calculated minimum temperature margins for the 6 double layers with comparison with the reference case (c).

Looking at the temperature profiles (Figure 11b) and temperature margins (Figure 11c) with respect to the current sharing temperature, the double layer DL5 is the most critical: the temperature margin of 1.5 K is reached at the end of the conductor length. The other DLS have temperature margin higher than 1.5 K up to 2.0

K for DL3 and DL4. One has to note that in the reference case (4.5 K and 1 bar pressure drop), DL2, DL5 and DL 6 do not comply with a temperature margin of 1.5 K. The impact of the inter-layer coupling (Figure 11a) can explain the different results obtained with the cooling scheme with independent circuit for each double layer. The heat loads are re-distributed and DL1 has lower heat load, whereas DL5 and DL6 have higher heat loads.

4.2 Pancake design

Table 7 shows the optimization results for WP3, based on a model including the 8 double pancakes. As the load distribution has been assumed the same for the 16 pancakes, only one hydraulic length of a pancake has been modelled. The refrigeration loads have been obtained by multiplying by 16 the results obtained for one pancake. The optimized cooling scheme would supply helium at 4.3 K, with a pressure drop of 0.2 bar. It would reduce the refrigeration power by -46% compared to the reference case (4.5 K and 1 bar).

Table 7: Optimization results for WP3

ΔP (bar)	0,20
T_{inlet} (K)	4,3
$P_{refr,\ reference}$ (W)	387
$P_{refr,\ optimized}$ (W)	207
Power saving (%)	-46
Heat loads (W)	164

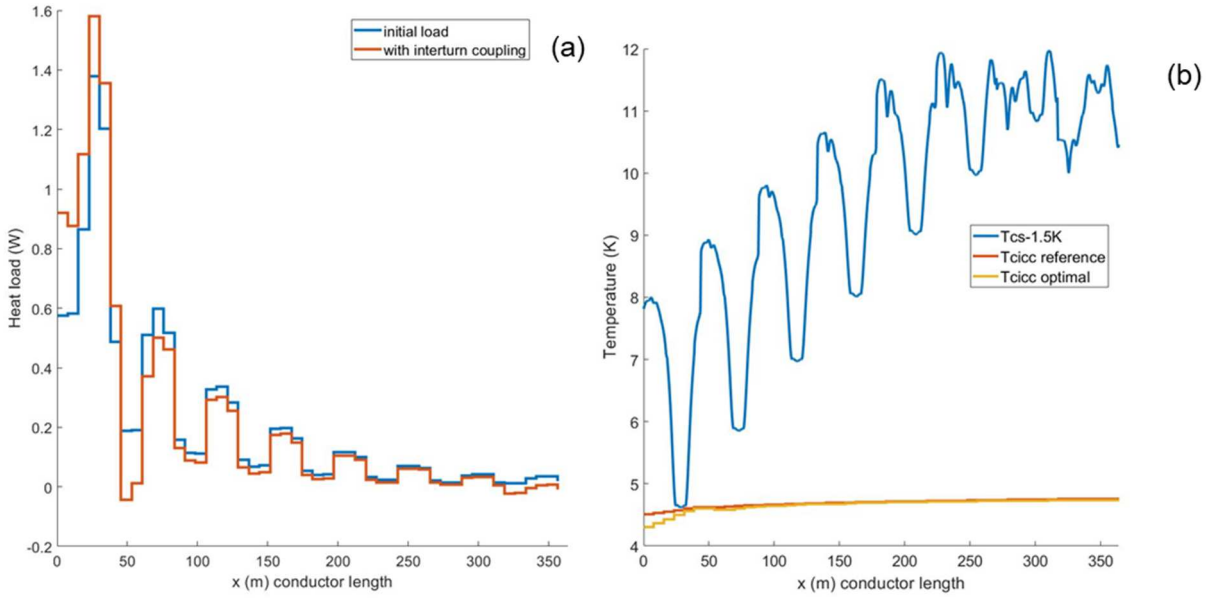

Figure 12: Optimization results for WP3: heat load repartition (a), conductor temperature profile for the pancake with comparison with the reference case (c).

Looking at the temperature profile with respect to the current sharing temperature, the temperature margin of 1.5 K is reached in the first 50 meters (1st turn) of the conductor length (Figure 12b). The remaining part of the conductor length has higher temperature margin up to 12 K. On can visualize the 8 turns of the hydraulic length. The impact of the inter-turn coupling (Figure 12a) is shown on Figure a: the heat loads are re-distributed with higher loads in the first 50 meters. The pancake design features some large temperature margin for a large amount of the conductor length. A dedicated cooling scheme could be devised to optimize the refrigeration power, in order to comply with the critical temperature constraint located in the first 50 meters of the conductor length.

4.3 Summary

Table 8 summarizes the optimization results presented in the previous section, for the three TF winding pack designs, resulting in three different sets of optimized cooling parameters (ΔP, $T_{inlet,CICC}$). They would induce different refrigeration requirements. The optimized refrigeration powers range from 229 W (WP1) to 271 W (WP2). The ranking is completely modified when the comparison is made with the ideal refrigeration power at

300 K: the WP3 design features the lowest ideal refrigeration power with 328 kW, whereas the WP1 and WP2 designs show ideal refrigeration closed to 400 kW. Besides, one can expect to investigate different cryo-distributions and different cryoplant architectures for the three sets of optimized parameters, so the total real refrigeration power at 300 K may change again the order, depending on the efficiency of the refrigeration processes. One main conclusion from the table 10 is related to the reference cooling parameters (T_{inlet} =4.5 K, ΔP=1 bar): they do not correspond to the calculated parameters to minimize the ideal refrigeration power. Some potential power saving of -30% and -46% has been estimated for WP1 and WP3 respectively. WP2 requires +25% ideal refrigeration power in order to become compliant with the temperature margin of 1.5 K.

Table 8: Summary table for the comparison for the optimization results obtained for WP1, WP2 and WP3

	WP1	**WP2**	**WP3**
ΔP (bar)	0.48	1.0	0.20
Mass flows (g/s)	~ 1700	~ 800	~ 1500
$T_{inlet,CICC}$ (K)	4.6	4.05	4.3
$P_{refr,\ reference}$ (W)	342	217	387
$P_{refr,\ optimized}$ (W)	229	271	207
Total Ideal Power $P_{ideal,\ optimized}$ (kW)	402	403	328
Power saving (%)	-33	+ 25	-46
Heat loads (W)	186	167	164

Figure 13 shows the refrigeration power sharing between the different contributors, with a comparison between the reference and optimal case. For all the three TF conductor designs, the same amount of nuclear heat loads have been assumed. Only WP1 model has included some additional loads due to the joint resistance. The contribution of the cryo-machines (cold compressor and cold circulator) can be compared between the three TF conductor designs. For WP1 and WP3, the reduction of pressure drop from 1 bar to respectively 0.48 bar and 0.2 bar, leads to a significant reduction of the cold circulator pumping power, despite the increased mass flow. For WP2, to become compliant with the 1.5 K temperature margin, the cold compressor pumping load is increased to pump down the temperature bath down to 4.05 K.

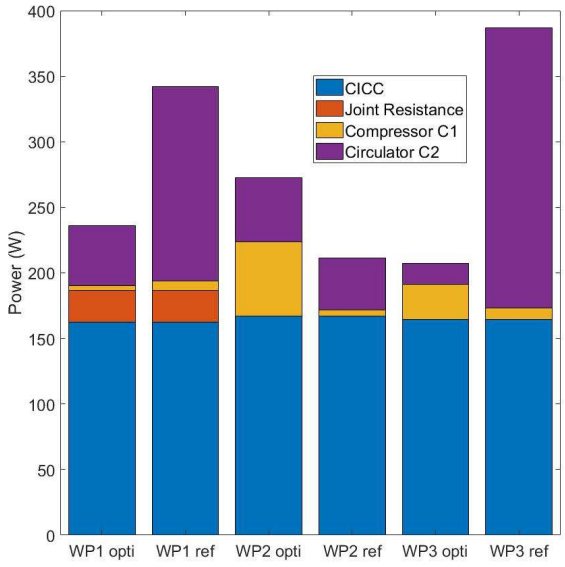

Figure 13: Comparative refrigeration load repartition for WP1, WP2 and WP3

5 Conclusions and perspectives

A methodology has been presented for optimizing the cooling parameters of the TF magnets, featuring layer wound or pancake wound conductors. This methodology relies on two sub-models. The first part includes a 1D conductor model with thermal inter-turn and inter layer couplings allowing a good representation of the thermal hydraulic behavior and of the heat load distribution along the conductor length. This first part has been thoroughly cross checked with parametric studies performed with other models (analytical and 2D models). The second part deals with a cryo-distribution model, consisting in a supercritical helium loop and the interface with the cold end of the refrigerator. The combination of the two parts leads to an optimization model, which allows to perform calculation loops on ($\Delta \boldsymbol{P}, \boldsymbol{T_{in,\,CICC}}$) in order to minimize the total refrigeration load, with a given temperature constraint on the temperature margin (1.5 K in the present study). The methodology has been applied on the 2015 DEMO TF conductor designs WP1, WP2 and WP3 assuming stationary neutron heat to assess a maximum temperature margin of 1.5 K. Additional heat load contribution (radiation and conduction) would need to be further investigated in the future. However, several outcomes can be drawn from the comparative results. The three TF designs have different optimized cooling parameters (ΔP, $T_{inlet,CICC}$), with inlet temperature for the conductor ranging from 4.05 K (WP2) to 4.6 K (WP1), with pressure drop ranging from 0.2 bar (WP3) to 1.0 bar (WP2). These three sets of cooling parameters would induce different refrigeration requirements for the cryogenic system specification. Not only the ideal refrigeration power is impacted, but the cooling requirements (ΔP, $T_{inlet,CICC}$) could lead to different architectures for the cryo-distribution and the cryoplant [22]. For instance, lower inlet temperature for the conductor in the range of 4.0 K would address some modification in the cold compressor compression ratio and the number of compression stage may be adjusted accordingly.

One main outcome to highlight is related to the reference cooling parameters ($\Delta \boldsymbol{P}$ =1 bar, $\boldsymbol{T_{in,\,CICC}}$=4.5 K), commonly used at conceptual design for the LTS conductor for fusion, which then lead to cryogenic cooling requirements at the interfaces: pressure drops in the range of [0.9, 1.4] bar and supply temperatures in the range of [4.3, 4.5] K to include also the cryo-distribution pressure head and heat losses and some options for subcooling operation. The optimization tool shows that ($\Delta \boldsymbol{P}$ =1 bar, $\boldsymbol{T_{in,\,CICC}}$=4.5 K) are not the optimized parameters to minimize the ideal refrigeration power for the three TF designs of EU DEMO. Some potential power saving of -30% and -46% has been estimated for WP1 and WP3 respectively. WP2 requires +25% ideal refrigeration power in order to become compliant with the temperature margin of 1.5 K. The present article shows the relevance to use an optimization tool at the conceptual design phase for EU DEMO. As the down selection of the different conductor options would be needed, this optimization tool can be applied and adjusted to assess the thermal hydraulic behaviors of different conductors. The cryo-distribution aspects are much coupled to the conductor design, through the cooling parameters (ΔP, $T_{inlet,CICC}$), which has to be discussed at early stage for a global approach of the cryo-magnet system, leading to efficient processes and cost effective solutions.

6 Acknowledgements

This work has been carried out within the framework of the EUROfusion Consortium and has received funding from the Euratom research and training programme 2014-2018 and 2019-2020 under grant agreement No 633053. The views and opinions expressed herein do not necessarily reflect those of the European Commission.

References

[1] Overview of the DEMO staged design approach in Europe, G. Federici et al., Nuclear Fusion, Vol. 59, n° 6, 2019, Art. 066013.

[2] EU Progress in Superconductor Technology Development for DEMO Magnets, V. Corato et al, Fusion Engin. and Design, vol. 136, 2018, pp.1597–1604.

[3] The DEMO Magnet System – Status and Future Challenges, Fusion Engineering and Design, V. Corato et al., Fusion Engineering and Design, vol. 174, 2022, Art. 112971.

[4] Parametric Optimization of the CEA TF Magnet Design of the EU DEMO Updated Configuration", L. Zani et al., IEEE Transactions on Applied Superconductivity Vol.29, n°5, 2019, Art. 4201205.

[5] Mechanical analysis of the European DEMO central solenoid pre-load structure and coils, F. Nunio, et al., Fusion Engin. and Design Vol. 146 part A, 2019, pp.168–172.

[6] Thermal-hydraulic analysis of different design concepts of the LTS TF coil winding pack for EU-DEMO, M. Lewandowska, A.Dembrkowska, K.Sedlak, International Conference on Electromagnetic Devices and Processes in Environment Protection with Seminar Applications of Superconductors (ELMECO & AoS), 2017, pp. 1-4, doi: 10.1109/ELMECO.2017.8267763.

[7] Thermo-hydraulic analyses associated to a CEA design proposal for DEMO TF conductor, R. Vallcorba et al., Cryogenics, vol. 80 no. 3, 2016, pp. 317-324.

[8] Thermal–Hydraulic Test and Analysis of the ENEA TF Conductor Sample for the EU DEMO Fusion Reactor, R. Bonifetto et al., IEEE Trans. Appl. Supercon., vol. 28, No. 4, JUNE 2018, Art. No. 4205909.

[9] (SPC) CS and TF Winding Pack Design and Analysis, K. Sedlak, P. Bruzzone, report for MAG-2.1-T004 (EFDA_D_2MT93A).

[10] Report on TF Winding Pack Design and Analysis (Option 2 - WP2), L. Muzzi, V. Corato, C. Fiamozzi Zignani, A. Anemona, report for WPMAG-MCD-2.1-T005 D001 (EFDA_D_2N4ALB).

[11] CEA TF winding pack design", D. Ciazynski, A. Torre, report for WPMAG-MCD-2.1-T003 D003, (EFDA_D_2MV7UD).

[12] Optimization of the cooling capacity of the cryo-magnetic system for EU DEMO at the pre-conceptual design phase, F. Bonne, C. Hoa, J.M. Poncet, L. Zani, B. Lacroix, Q. LeCoz, V. Lamaison, Fusion Engineering and Design, September 2019, 146:2504-2508.

[13] Optimization of the overall Toroidal Field Coil cryo-magnetic system at the pre-conceptual design phase of the European DEMO fusion reactor, Sandra Varin et al, Fusion Engineering and Design, , vol. 172, 2021, Art. 112883.

[14] Simcryogenics: a library to simulate and optimize cryoplant and cryodistribution dynamics, Bonne, F., Bonnay, P., Hoa, C., Millet, F., Poncet, J.-M., Rousset, B., et al. IOP Conference Series: Materials Science and Engineering 2019.

[15] Fundamentals of Heat Exchanger Design, R.K. Shah, D.P. Sekulić, Wiley, New Jersey, 2003 (Table 7.6).

[16] Common Operating Values for DEMO Magnets Design for 2016, (2016), V. Corato, et al., Available at: https://scipub.euro-fusion.org/archives/eurofusion/common-operating-values-for-demo-magnets-design-for-2016-2.

[17] Friction factor correlation for CICC's based on a porous media analogy, M. Bagnasco, L. Bottura, M. Lewandowska, Cryogenics, vol. 50, pp. 711-719, 2010.

[18] Advanced definition of neutronic heat load density map on DEMO TF coils, L. Zani and U. Fischer, Memo for WPMAG-MCD-2.1/2.2/ 3.3, 2014, https://idm.euro-fusion.org/?uid=2MFVCA.

[19] Towards a multi-physic platform for fusion magnet design—Application to DEMO TF coil, Quentin Le Coz, Daniel Ciazynski, Benoît Lacroix, Sylvie Nicollet, François Nunio, Alexandre Torre, Roser Vallcorba, Louis Zani, Fusion Engineering and Design, Vol. 124, Pages 104-109 2017.

[20] Thermal-hydraulic analysis of LTS cables for the DEMO TF coil, M. Lewandowska, K. Sedlak, IEEE Trans. Appl. Supercond., vol. 24, no. 3, Jun. 2014, Art. 4200305.

[21] Conceptual design of the JT-60SA cryogenic system, V. Lamaison, J. Beauvisage, P. Fejoz, S. Girard, R. Gonvalves, R. Gondé, V. Heloin, F. Michel, C. Hoa, K. Kamiya, P. Roussel, J-C. Vallet, M. Wanner, and K. Yoshida, AIP Conference Proceedings 1573, 337 (2014).

[22] EU DEMO cryogenic system and cryo-distribution: pre-conceptual design for an optimal cooling of the superconducting magnets and the thermal shields, C. Hoa, V. Lamaion, M. Wanner, S. Ciattaglia, J-M. Bernardt, M. Roig, D. Till, B. Anseaume, 28th IAEA Fusion Energy conference, to be published in IAEA Nuclear Fusion journal 2021.